SUPPLEMENTARY INFORMATION

Optical anisotropy in single walled carbon nanotube thin films: Implications for transparent and conducting electrodes in organic photovoltaics

The fact that the SWNTs in sparse networks are likely to lay flat on the substrate surface should lead to different in-plane (//) and out-of-plane (⊥) components of the complex dielectric function at any photon energy, E:

$$\varepsilon_{//}(E) = \tfrac{1}{2} \cdot E \cdot [\sigma_o(E) + \sigma_e(E)] \qquad \varepsilon_{\perp}(E) = E \cdot \sigma_o(E) \tag{1}$$

The method of Strachan [18] to extract the optical constants of thin films requires ellipsometry measurements at a constant incidence angle (θ) of the same film deposited on different isotropic substrates with different dielectric functions, ε_{0i}. The optical strengths, σ_o and σ_e, are then related to the measured ellipsometry angles Ψ and Δ by [18]:

$$\frac{\rho_i - \rho_{0i}}{\rho_i} = f \cdot \frac{8\pi j \cdot d \cdot E}{hc} \cdot \frac{\sigma_o - \varepsilon_{0i} \cdot \sigma_e}{(\varepsilon_{0i} - 1) \cdot (\cos^2\theta - \sin^2\theta) \cdot \varepsilon_{0i}} \tag{2}$$

where *h* and *c* are the Planck's constant and the speed of the light, *f* is the fraction of the substrate covered by the discontinuous film, *d* is the film thickness, $\rho_i = \tan(\Psi_i)\cdot\exp(j\Delta_i)$ for each of the i = 1,…,*m* covered substrates under investigation, while $\rho_{0i} = \tan(\Psi_{0i})\cdot\exp(j\Delta_{0i})$ can be determined from measurements on bare substrates prior to film deposition. Therefore, at each photon energy (E), eq. (2) represents a system of *m* independent linear equations with two unknowns (σ_o and σ_e and the components of the complex dielectric functions, which are related to the optical strengths by means of eq. 1). *m*–2 equations can therefore be used to determine the uncertainty in the procedure. This method is well suited for our case since the reproducibility of the same film on different substrates is not a major limitation for the SWNT thin film method utilized here. Furthermore, our analysis method, which takes into account the dipolar interactions between different oscillators within the effective medium theory, is much more general than that of eq.(2) (which strictly holds only at *f* <<

1 and neglects the dipole-dipole interaction of the optical oscillators [19]). We have extracted the in- and out-of-plane components of the complex dielectric function of our thin films through this more general numerical procedure.

The ellipsometry data on the different substrates were then simulated using the Jobin-Yvon PsiDelta software by means of (a) anisotropic and (b) isotropic models. Within the anisotropic model, each component (in- and out-of-plane) of the complex dielectric response of the SWNTs was assumed to be the superposition of a Lorentzian oscillator (taking into account the π-π* interband transitions) and a Drude background (for considering the intraband contribution to the optical properties related to the presence of free electrons in percolating networks of metallic SWNTs) as follows:

$$\varepsilon_{//} = \varepsilon_{\infty} + \frac{I_{//}}{E_{\pi//}^2 - (E + j\Gamma_{\pi//})^2} + \frac{E_{pl//}^2}{-E^2 + j\Gamma_{pl//}E} \qquad \varepsilon_{\perp} = \varepsilon_{\infty} + \frac{I_{\perp}}{E_{\pi\perp}^2 - (E + j\Gamma_{\pi\perp})^2} \tag{3a}$$

Where I, E_{π} and Γ_{π} are the intensities, maximum transition energies and broadening parameters for the in-plane (//) and out-of-plane (⊥) components of ε, respectively; E_{pl} is the plasmon energy and Γ_{pl} is the plasmon broadening. Within the isotropic model, the dielectric response of the SWNTs was assumed to be the superposition of two Lorentzian oscillators and a Drude background:

$$\varepsilon = \varepsilon_{\infty} + \sum_{i=1}^{2} \frac{I_i}{E_{\pi i}^2 - (E + j\Gamma_{\pi i})^2} + \frac{E_{pl}^2}{-E^2 + j\Gamma_{pl}E} \tag{3b}$$

In order to consider the discontinuous character of our SWNT thin films and the presence of voids, the effective dielectric functions of the SWNT thin films ($\varepsilon_{eff,//}$ and $\varepsilon_{eff,\perp}$ or ε_{eff}) were determined for both cases from the dielectric responses of the SWNTs ($\varepsilon_{//}$ and $\varepsilon_{\perp}$ or ε) within the Bruggeman effective medium theory [20]. The SWNT thin films were modeled as being composed of a volume fraction (*f*) of SWNTs and a complementary fraction (1–*f*) of voids. Subsequently, *f*, the film thickness (*d*), and the Lorentzian and Drude parameters in eqs.(3) were determined by

comparing the calculated and measured values of Ψ_i and Δ_i by means of χ-square minimization.

We quantitatively demonstrate this by extracting the complex dielectric function of our SWNT thin films and ITO from the ellipsometry data in figures S1a (films on glass) and S1b (films on Si). Lines in figures S1a-b represent best-fits of the experiments achieved by means of the isotropic [eq.(3b) (dotted line)] and anisotropic [eq.(3a) (solid line)] models. It can be seen that both eqs.(3a) and (3b) satisfactorily fit the experimental trends of the ellipsometric angles, Ψ_i and Δ_i (Fig. S1a-b), when proper values of the complex dielectric functions are assumed. However, when the dielectric functions obtained from Ψ_i and Δ_i are used to calculate the transmittance on glass, the trend from the isotropic model [eq.(3b)] is unable to reproduce the strong variations in the measured data as a function of θ. In Figure 1b of the MS, the fits from the two models for the transmittance data at E = 2.25 eV are shown. It can be seen that the solid lines (representing the anisotropic model) describe the data much better than the dotted lines (calculated assuming an isotropic material). Thus, although our ellipsometry data can be modeled by both equations (3a) or (3b), the transmittance of the SWNT thin films requires an anisotropic description.

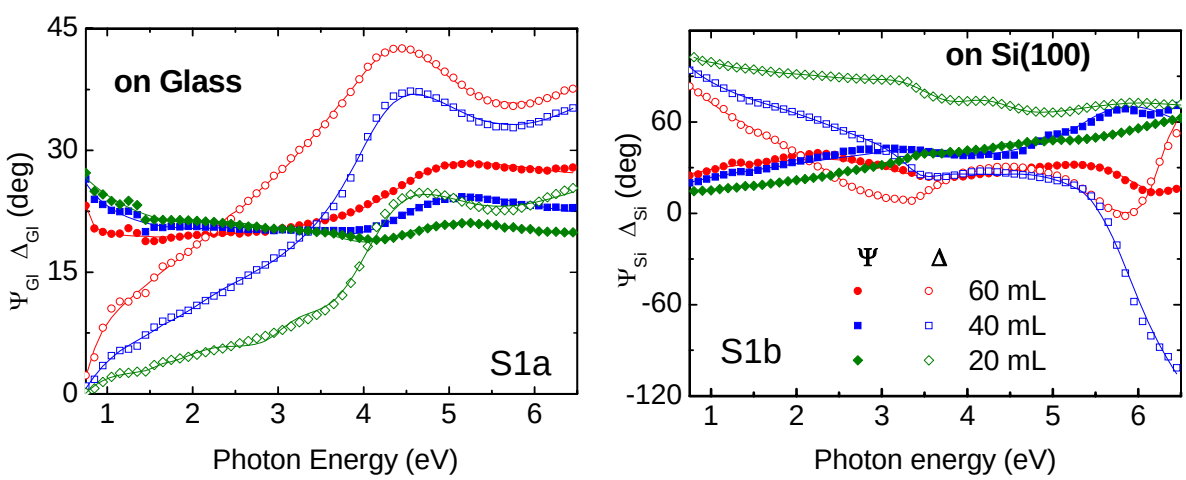

Figure S1: Ellipsometry angles Ψ_i and Δ_i (θ = 70°) of our films on (S1a) glass and (S1b) silicon substrates, respectively. Continuous lines are fits by eq.(3a).

We now discuss the physical reasons leading to anisotropy in SWNT thin films. The optoelectronic properties of individual SWNTs having (n,m) chiral indices are controlled by π-electrons giving rise to ν = 1,…,n bands of the form [13]:

$$\in_{\nu}^{(c/v)}(k) = \pm\beta\sqrt{1+4\cdot\cos\left(\frac{2\pi\nu}{n}-\frac{n+2m}{2n}kl\right)\cdot\cos\left(\frac{kl}{2}\right)+4\cos^{2}\left(\frac{kl}{2}\right)} \quad (5)$$

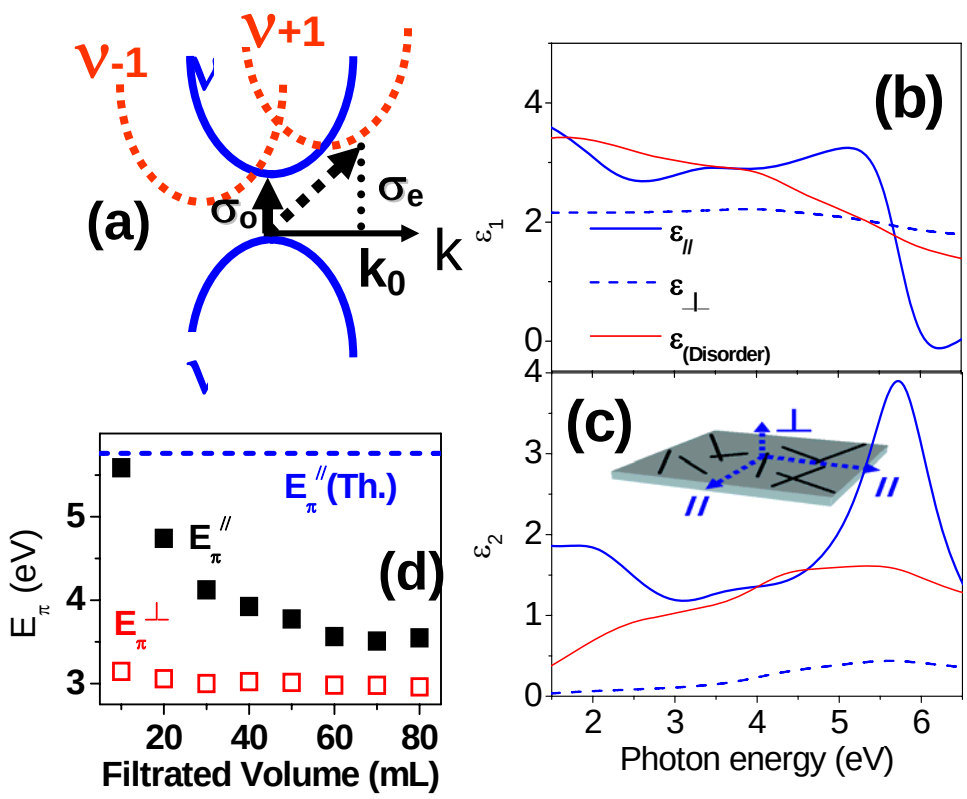

Figure S2: (a) Model used for determining the in- and out-of-plane direct optical transitions accordingly to Tasaki et al [13] [Eqs.(6)]. (b and c) Tight binding simulations of in-plane and out-of plane real (ε_1, panel b) and imaginary (ε_2, panel c) parts of the complex dielectric functions, leading to $E_{\pi//} \approx 5.76$ eV when selection rules are applied as in eqs. (6) and a much lower value of $E_{\pi} \approx 4$ eV eV when selection rules are released by disorder, explaining, at least qualitatively, the redshift of $E_{\pi//}$ shown in panel (d).

where $\beta \approx 2.88$ eV, $l \approx 2.1$ Å is the unit cell size in the reciprocal space and the ± signs refer to the conduction (c) π*-bands and the valence (v) π-bands, respectively. Direct optical transitions have to obey the conservation of momentum and energy. Energy conservation requires transitions at photon energies $E = \in_{\mu}^{(c)}(k) - \in_{\nu}^{(v)}(k')$. Using the notation introduced by Tasaki et al [13] in eq.(5), momentum is conserved only for $\pi \rightarrow \pi^*$ transitions involving [13]:

$$\mu = \nu \text{ and } k' = k \text{ in axial (e) direction} \tag{6a}$$

$$\mu = \nu \pm 1 \text{ and } k' = k + k_0 \text{ in tangential (o) direction} \tag{6b}$$

Where $k_0 = 3\cdot(n+2m)\cdot l/\pi D_{n,m}$ is the change in momentum induced by the curvature, which depends on $D_{n,m}$, the tube diameter. The processes summarized in eqs. (6) are depicted in Figure S2a.

Optical transitions are especially strong between two Van Hove (VH) singularities of the electronic density of states (DOS), which correspond to null second derivatives of $\in_{\nu}^{(c/v)}(k)$. Furthermore the magnitude of the dipole matrix elements control the intensity of the optical transitions. Diagonal matrix elements, describing the optical transitions from valence to conduction bands having the same index ($\mu=\nu$) are particularly strong [13]. Thus, such transitions (E_{ii}), involving light propagating along the tube axis, are intense (see Fig. S2a) which leads to large values of σ_e and via eq.(1) of $\varepsilon_{//}$.

In contrast, the optical absorption of an individual SWNT is weaker in tangential direction as it generally occurs (see Fig. S2a) from $E_{ii\pm1}$ transitions involving non diagonal ($\mu\neq\nu$) dipole matrix elements. Since most SWNTs lay flat on the substrate with their axes parallel to the substrate surface, such transitions are the only ones occurring in out-of-plane direction (see eq. 1) and they are responsible for the lower imaginary parts of the complex dielectric function in that direction. We have performed a simple tight binding estimation of the complex dielectric function of SWNT thin films in the framework of eq. (5) and (6) for an ensemble of (n,m) SWNTs corresponding to

those produced by the HipCO method [21]. The computer program implementing such a calculation and its description are available as supplementary material.

The resulting calculated dielectric constants are shown in Figure S2b-c. Although our calculations are able to successfully reproduce the in- and out-of-plane components of ε (having energy maxima at $E_{\pi//} \approx 2\beta$ and a much broader absorption feature for $\varepsilon_{\perp}$ compared to $\varepsilon_{//}$) they assume that all the nanotubes are perfectly straight, far from experimental reality. More accurately, as the density of SWNT increases (i.e. as the filtrated volume of the suspension is increased from 20 mL to 80 mL), the SWNT networks become more constrained and disorder becomes important. The increase of disorder involves curvature and twisting of the SWNTs, even though they still preferentially lay flat to the substrate. Curving the tube axes leads to the release of the selection rules within each SWNT and optical transitions become equally permitted for more values of k and k'. In the absence of selection rules, Tauc [22] showed that the imaginary part of the dielectric function represents the joint density of occupied and unoccupied states. In this case, the energy maximum for ε_2 (disordered) shifts at lower energies than $2\beta \approx 5.76$ eV, corroborating the observed red-shift of $E_{\pi//}$ with increasing network density in our films (see Figure S2d). In contrast, the out-of-plane energy maximum for π-π^* transitions is strongly red-shifted even at the lowest SWNT network density, as can be seen in Figure 3d ($E_{\pi\perp} \approx 3$ eV). This could indicate an earlier influence of disorder in such direction as a consequence of the presence of a few curved SWNTs not laying perfectly flat on the substrate.